

# Local magnetostrictive response of small magnetic entities in artificial Fe–Cr composites

Nikolay I. Polushkin<sup>a)</sup>

*Institute for Physics of Microstructures of RAS, 603950 GSP-105 Nizhni Novgorod, Russia*

J. Wittborn, C. Canalias, and K. V. Rao

*Department of Materials Science, Royal Institute of Technology, SE-10044 Stockholm, Sweden*

A. M. Alexeev and A. F. Popkov

*State Research Institute of Physical Problems, NT-MDT, 103460 Moscow, Russia*

(Received 12 April 2002; accepted for publication 21 June 2002)

Nanoscale ferromagnetic entities are directly patterned in superparamagnetic Fe–Cr layers by interfering laser beams. To characterize the formed entities, in addition to the conventional methods, we used a technique for magnetic imaging based on the atomic force microscopy (AFM) with nonmagnetic tips and an ac magnetic field applied *in situ*. The observed AFM dynamic response is interpreted in terms of magnetostriction and a related quantity, the ac susceptibility. © 2002 American Institute of Physics. [DOI: 10.1063/1.1500783]

## I. INTRODUCTION

Artificially produced media composed of small magnetic entities have attracted considerable interest recently from the viewpoint of their potential application in data storage systems.<sup>1,2</sup> The features as small as 100 nm and less are patterned in thin magnetic films currently by means of multistep lithographic processes involving deposition and subsequent etching of a resist layer as the key technological operations. In our work, we use a simple effective and low-cost approach to such fabrication, namely, direct (resistless) patterning of small magnetic entities in alloyed layers of Fe–Cr type via laser-induced phase changes.<sup>3,4</sup> Various studies on nanocrystalline Fe-based alloys<sup>5–7</sup> emphasize the dominating role of superparamagnetic Fe-rich clusters in the behavior of the entire system, so the alloys do not exhibit long-range magnetic order up to a high Fe content (70–75 at. %). In the Fe<sub>70</sub>Cr<sub>30</sub> alloys subjected to laser annealing, we revealed arising of a room-temperature ferromagnetic phase, in which the saturation magnetization was close to that in bulk Fe.<sup>4,8</sup> It is believed that by laser annealing, the alloy components mix up in the liquid phase to yield, when cooled, a supersaturated solid solution with a high Curie temperature.<sup>9</sup>

In producing small magnetic features, the peculiarity of such processing is that the patterned features strongly depend on the parameters of a heating pulse. A high intensity and a very long pulse duration cause blurring of the modified regions. To characterize such systems unambiguously will require the use of different techniques such as the magnetic force microscopy (MFM) and magnetometry. In addition to these, we here employ a technique for magnetic imaging, namely, detection of a local magnetostriction response by a nonmagnetic probe of an atomic force microscope (AFM) in an ac field applied *in situ*.<sup>10</sup> These measurements performed at various orientations of an ac field and the magnetization of

the entities allow us to identify locations that have different magnetic properties. It is also expected that the spatial resolution of this technique can be comparable with that typical of AFM. The observed behavior of the amplitude of dynamic surface oscillations can be explained by the magnetostriction effect that is due to the field-induced precession of magnetic moments.

## II. EXPERIMENTAL TECHNIQUES

The Fe–Cr alloyed layers for subsequent processing were prepared on Si substrates by a 1.06  $\mu\text{m}$  Nd:YAG laser ablation of separate Fe and Cr targets. As our ferromagnetic resonance (FMR) studies showed,<sup>8</sup> the as-prepared Fe<sub>70</sub>Cr<sub>30</sub> mixtures did not possess any magnetic response at room temperatures, whereas a well-defined FMR signal appeared after irradiation by a one nanosecond laser pulse with the fluence of about 0.1 J/cm<sup>2</sup>.

To produce small features upon this basis, the mixtures are irradiated by four interfering beams of a XeCl ( $\lambda = 308$  nm) narrowband (0.04 cm<sup>-1</sup>) excimer laser having a pulse duration of 10 ns. A coherent addition of four beams incident in two mutually orthogonal planes results in two-dimensional patterns of interference maxima and minima of the light intensity with a periodicity of  $\lambda/\sqrt{2} \sin \theta$ , where  $\theta$  is the angle of incidence. The patterned regions can have an anisotropic shape if (i) the beams are incident at different angles and (ii) the thermal diffusion length ( $\sim 100$ – $200$  nm) is small compared to the areas of the highest laser intensity in the interference maxima. The details of the interferometric laser annealing are given elsewhere.<sup>11</sup>

In order to induce surface oscillations of patterned samples, an ac magnetic field with the frequency,  $f$ , in the range from 30 to 100 kHz, and with the amplitude not more than a few Oe is applied *in situ*. The surface oscillations transferred to the probe that scanned in the contact mode. The amplitude of the surface oscillations was measured in

<sup>a)</sup>Electronic mail: nip@ipm.sci-nnov.ru

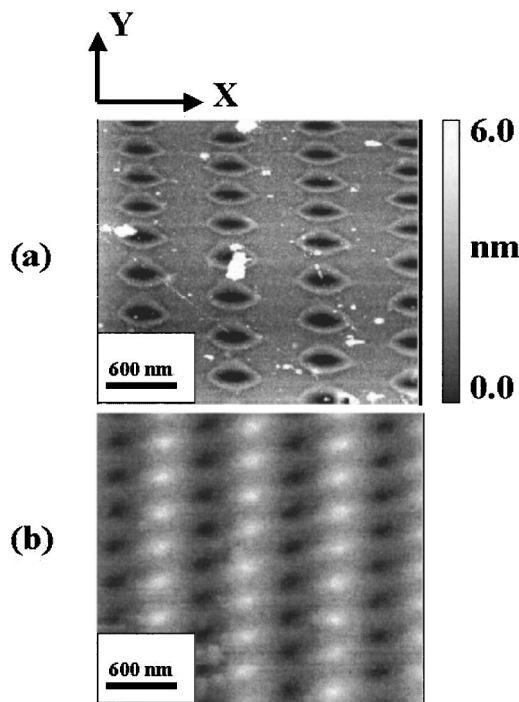


FIG. 1. AFM topographic (a) and MFM (b) images of a 15 nm thick Fe–Cr layer patterned by means of interfering laser beams. The MFM image has been collected after magnetizing the sample in the direction along the  $X$  axis and indicates locally induced modifications in magnetic properties.

arbitrary units by using a lock-in amplifier with the  $2\omega$  ( $\omega = 2\pi f$ ) mode for magnetostriction.

It is important that, for detecting the signal, the frequency was chosen so as to have  $2\omega$  close to the resonance frequency of the cantilever. The studies of the AFM dynamic response were performed on a “Burleigh” scanning probe microscope. Using this apparatus, we had an opportunity to apply an alternating magnetic field *in situ* both in the sample plane and perpendicular to it.

### III. RESULTS

Figure 1 shows [Fig. 1(a)] a topographic (AFM) image of the patterned surface of a 15 nm thick layer of Fe<sub>70</sub>Cr<sub>30</sub> (Fe–Cr) and [Fig. 1 (b)] its MFM image collected after the sample was magnetized by applying the magnetic field of about 1.0 kOe in the direction along the  $X$  axis. These AFM/MFM images have been obtained on a Solver P47 apparatus (NT-MDT). The AFM image shows the craterlike regions located in the interference maxima. The crater shape is a result of the film melting in the interference maxima and the Fe–Cr liquid being expelled by a radial vapor pressure<sup>12</sup> from the center to the periphery. The Fe–Cr liquid viscosity is high enough to prevent the formed surface profile from smoothing out over the cooling times which are of the order of  $10^{-7}$  s. The width of the crater walls (light contrast around the craters) is of  $\sim 50$  nm, and their height is of  $\approx 10$  nm. The crater features depend on the laser fluence, so the crater depth can reach the film thickness at fluence above 0.5 J/cm<sup>2</sup>. The MFM image in Fig. 1 (b) shows a periodic structure of dipoles: The dark and light contrast in the pattern indicate the poles of the ferromagnetic regions which are

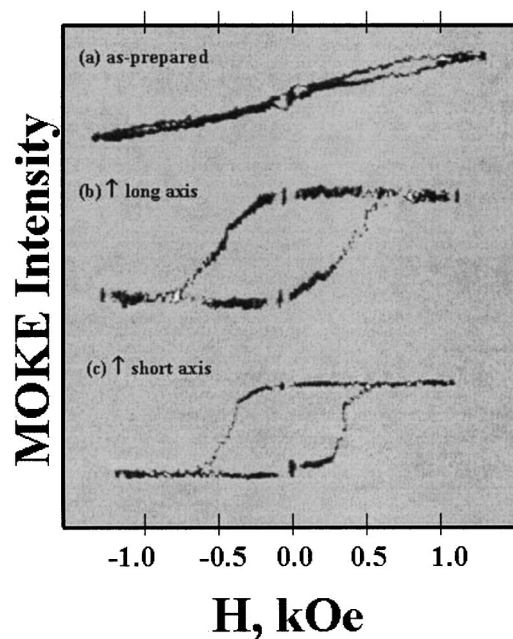


FIG. 2. (a) Magnetization curve of an as-prepared Fe<sub>0.7</sub>Cr<sub>0.3</sub> layer. (b and c) Hysteresis loops of a patterned sample, obtained at different directions of the external field,  $\mathbf{H}$ , with respect to the axes of the crater: along the long axis (b) and along the short axis (c).

fully polarized in the same direction. This observation provides the first and clear evidence for local modifications in the magnetic properties of the alloys under study.

Laser-induced transformations in Fe–Cr films can also be observed by the longitudinal magneto-optical Kerr effect (MOKE). Figure 2 shows MOKE intensity as a function of a static magnetic field,  $H$ , for an as-prepared Fe–Cr film [Fig. 2(a)] and the patterned film [Figs. 2(b) and 2(c)] with the craters such as in Fig. 1. In the latter case, the MOKE intensity was measured for two different directions of  $\mathbf{H}$ : Along the long axis of the craters [Fig. 2(b)] and along their short axis [Fig. 2(c)]. We see that the magnetization curves of the patterned film possess the hysteresis features that are typical of ferromagnets, whereas the as-prepared film exhibits a superparamagneticlike (anhysteretic) behavior with a relative low static susceptibility,  $(dM/dH)_{H \rightarrow 0}$ , and some magnetization saturation at fields above 1.0 kOe. As seen, for both the field directions, the hysteresis loops of the patterned film indicate a nearly full moment in the remanent state; however, there is some magnetic anisotropy which probably results from the competition between the demagnetizing fields inside the craterlike entities and the effects of superparamagnetic environment.<sup>4</sup>

Figure 3 shows a topographic image [Fig. 3(a)], obtained in the same mode as in Fig. 1(a), versus the images of the amplitude of the oscillations of the probe [Figs. 3(b) and 3(c)], arising due to the field-induced surface oscillations, obtained at  $2\omega$  for some value of the ac field,  $h_{ac}$ . The dynamic images were collected after prior magnetization of the sample up to saturation along the long axis [Fig. 3(b)] as well as along the short axis [Fig. 3(c)] of the craters. It is remarkable that the features of the crater observed in the conventional and dynamic modes are in direct relationship.

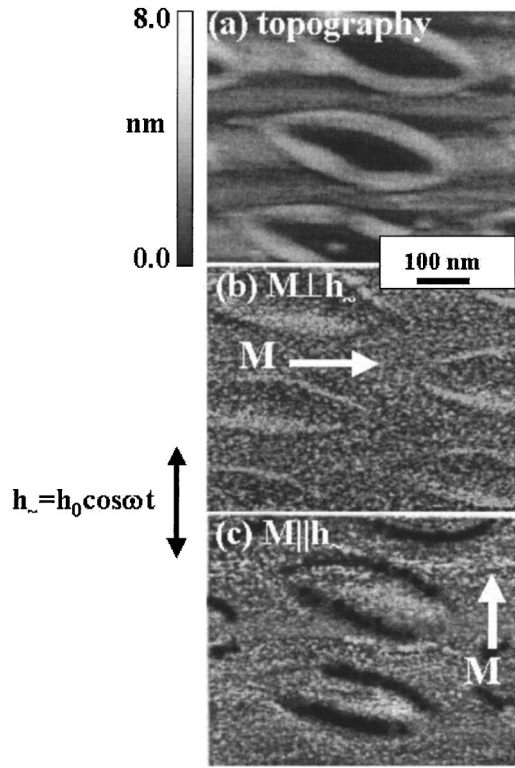


FIG. 3. AFM topographic (a) and the corresponding images of the dynamic response, collected at  $f = 50.1$  kHz after prior magnetization along the long axis (b) and the short axis (c) of craters. The orientation of the ac field and the magnetization of the crater  $\mathbf{M}$ , are indicated by arrows.

This similarity may have a simple explanation, considering that the crater walls are the most distinctive topographic feature and that they also correspond to the maximum of the ferromagnetic matter which naturally can have the largest magnetic response. As seen from Figs. 3(b) and 3(c), the oscillation amplitude in the crater walls depends on the mutual orientation of the ac field and the static craters' magnetization,  $\mathbf{M}$ . When  $\mathbf{h}_\perp$  is applied parallel to  $\mathbf{M}$ , the wall oscillations are even smaller than those of the surrounding medium [Fig. 3(c)]. However, we observed some enhancement of the wall oscillations after applying the ac field in the film plane and perpendicular to the magnetization. In the latter case, the oscillations became larger than those of the surrounding medium [Fig. 3(b)]. Finally, there was no difference detected in the dynamic response of the craters and surrounding matrix at applying an out-of-plane ac field.

#### IV. DISCUSSION

We shall explain the observed behavior of the local dynamic response and its dependence on the ac-field orientation in terms of field-induced magnetostriction effects. Such a suggestion, firstly, is supported by our observations of vanishing of the AFM dynamic response of a nonmagnetic Fe–Cr layer with patterned craters. Moreover, such a response in the magnetic samples is observable at  $2\omega$ . The magnetostrictive deformations, as known,<sup>13</sup> are quadratic in the direction cosines of the magnetization vector, so the deflection of the AFM tip at the second harmonics can be associated with the magnetostrictive response under the probe

scanning in the contact mode. The magnetostrictive deformations can be expressed via the components of the ac susceptibility,  $\chi$ ,

$$u_{ij} = \frac{\lambda_{1(2)}}{M^2} \chi_{ik} \chi_{jl} h_k h_l \cos^2 \omega t, \quad (1)$$

where  $\lambda_{1(2)}$  are the dimensionless magnetostrictive constants and  $h_{k(l)}$  are the components of the ac field. It is important to point out that the ac susceptibility is the amplitude of precession of the magnetization around the easy axis of magnetization. When  $\mathbf{h}_\perp$  is parallel to the magnetization, the precession of magnetic moments does not arise. This expectation agrees qualitatively with our experimental observations of the vanishing of the local response under such an orientation of  $h_\perp$  [Fig. 3(c)]. For the perpendicular orientation of  $\mathbf{h}_\perp$  with respect to the direction of  $\mathbf{M}$ , taking into account that the demagnetizing factor along the normal (Z axis) to the film plane (X–Y) is close to unity, one can obtain the solution of the Landau–Lifshitz equation for the motion of the magnetization in the following form

$$\chi_{yy} \approx \frac{4\pi\gamma^2 M^2}{\omega_0^2 - \omega^2}, \quad \chi_{zy} = \frac{\gamma M \omega}{\omega_0^2 - \omega^2}, \quad (2)$$

under the in-plane orientation of  $\mathbf{h}_\perp$  along the Y axis, and

$$\chi_{zz} = \frac{4\pi\gamma^2 M^2 \Delta N}{\omega_0^2 - \omega^2}, \quad \chi_{yz} = \frac{\gamma M \omega}{\omega_0^2 - \omega^2}, \quad (3)$$

under the out-of-plane orientation of  $\mathbf{h}_\perp$ . In these equations,  $\omega_0 = 4\pi\gamma M \sqrt{\Delta N}$  is the natural frequency of the system,  $\Delta N$  is the difference between the demagnetizing factors along the long and short axes of the entities, and  $\gamma$  is the gyromagnetic ratio. For our experimental conditions,  $\omega$  is infinitesimal compared with  $\gamma M$  and  $\omega_0$  that have values of the order of 10 GHz. Therefore, one can neglect  $\omega$  in the denominator of Eqs. (2) and (3), and it is difficult to observe the effects of magnetic resonance in these experiments. Besides, since  $\Delta N \ll 1$ , the oscillations caused by the out-of-plane ac field are much weaker than those arising under the in-plane ac field. This is also compatible with our experimental observations.

In accordance with Eqs. (1)–(3), one can roughly estimate the amplitude of field-induced surface oscillations, which is of  $\sim 10^{-5}$  nm ( $\lambda_{1(2)} \sim 10^{-5}$ ,  $h_{y(z)} \sim 10$  G, and  $M \sim 10^3$  G). In the contact mode that corresponds to the regime of repulsive forces<sup>14</sup> which are proportional to  $r_0^{-13}$ , where  $r_0$  is the spacing between the tip and the sample surface, such surface oscillations can cause enhanced oscillations of the tip with the amplitude of  $\sim 0.1$  nm, given the proximity of the double frequency of the ac field to the resonance frequency of a high- $Q$  cantilever ( $Q \sim 100$  in air).<sup>15</sup>

Thus, such a locally observed dynamic response may indicate the regions with different susceptibilities, and the AFM technique presented here can be used as a tool for visualizing magnetic entities. As applied to the patterned Fe–Cr layers, the AFM technique presented here is found to indicate the laser-induced formation of ring-shaped magnets. Indeed, the magnetic properties of the rings (crater walls) differ from those of the intracrater regions and the intercrater

medium. In an applied ac magnetic field, the oscillation amplitude of the crater walls strongly depends on the orientation of the ac field with respect to the direction of the magnetization of the entities. Our conclusion hereof is that in the patterned films, the (ferro)magnetic phase is localized mainly within the crater rings in the topographic images. It is also interesting that the observed dynamic response can be even smaller than that of a surrounding matrix.

## V. CONCLUSIONS

We have fabricated regular arrays of ferromagnetic craterlike entities in superparamagnetic Fe–Cr layers by employing interferometric laser annealing. Ferromagnetic ordering in the maxima of laser intensity is probably due to formation of a rapidly quenched solid solution having a high Curie temperature, instead of an initially granular superparamagnetic medium. Squeezing out the melted liquid by a radial vapor pressure leads to the formation of ring-shaped entities. Our studies of the formed entities by MFM and MOKE show that the entities are ferromagnetic and remain in their single-domain state after magnetizing up to saturation. Some new kind of information about this object can be obtained by probing it with a nonmagnetic probe of an AFM in an ac field applied *in situ*. We found that the crater walls, where the ferromagnetic matter is mostly concentrated is a patterned feature whose dynamic response is most sensitive to variations of the orientation of the magnetization of the entities or the ac field. The observed AFM dynamic response and its behavior can be explained in terms of magnetostrictive deformations and the ac susceptibility.

## ACKNOWLEDGMENTS

The work was partially supported by the RFBR Grant (No. 01-02-16445). The authors wish to thank Yu. K. Ver-

evkin and V. N. Petryakov, who are with the Institute of Applied Physics of RAS, for providing excimer laser facilities. One of the authors (N.I.P.) is grateful to the management of the Royal Institute of Technology for hospitality during his stay at the Department of Materials Science.

- <sup>1</sup>S. Y. Chou, *Proc. IEEE* **85**, 652 (1997).
- <sup>2</sup>R. M. H. New, R. F. W. Pease, and R. L. White, *J. Vac. Sci. Technol. B* **13**, 1089 (1995).
- <sup>3</sup>M. Zheng, M. Yu, R. Skomski, S. H. Liou, D. J. Sellmyer, V. N. Petryakov, Y. K. Verevkin, N. I. Polushkin, and N. N. Salashchenko, *Appl. Phys. Lett.* **79**, 2606 (2001).
- <sup>4</sup>A. M. Alekseev, Y. K. Verevkin, N. V. Vostokov, V. N. Petryakov, N. I. Polushkin, A. F. Popkov, and N. N. Salashchenko, *JETP Lett.* **73**, 192 (2001).
- <sup>5</sup>C. Schwink, K. Emmerich, and U. Schulze, *Z. Phys. B* **31**, 385 (1978).
- <sup>6</sup>K. Takanashi, T. Sugawara, K. Hono, and H. Fujimori, *J. Appl. Phys.* **76**, 6790 (1994).
- <sup>7</sup>D. Babonneau, J. Briatico, F. Petroff, T. Cabioc'h, and A. Naudon, *J. Appl. Phys.* **87**, 3432 (2000).
- <sup>8</sup>N. I. Polushkin, S. A. Gusev, M. N. Drozdov, Y. K. Verevkin, and V. N. Petryakov, *J. Appl. Phys.* **81**, 5478 (1997).
- <sup>9</sup>O. Kubaschewski, *Iron-binary Phase Diagrams* (Springer, Berlin, 1982).
- <sup>10</sup>J. Wittborn, K. V. Rao, J. Nogues, and I. K. Schuller, *Appl. Phys. Lett.* **76**, 2931 (2000).
- <sup>11</sup>V. I. Bredikhin, Y. K. Verevkin, E. Y. Daume, S. P. Kuznetsov, O. A. Mal'shakova, V. N. Petryakov, N. V. Vostokov, and N. I. Polushkin, *Quantum Electron.* **30**, 333 (2000).
- <sup>12</sup>M. Allmen, *Laser-beam Interactions with Materials* (Springer, Berlin, 1987).
- <sup>13</sup>L. D. Landau, E. M. Lifshitz, and L. P. Pitaevskii, *Electrodynamics of Continuous Media*, 2nd ed. (Butterworth, Oxford, 1984).
- <sup>14</sup>E. V. Blagov, V. M. Mostepanenko, and G. L. Klimchitskaya, *Tech. Phys.* **44**, 970 (1999).
- <sup>15</sup>T. R. Albrecht, P. Grütter, D. Horne, and D. Rugar, *J. Appl. Phys.* **69**, 668 (1991).